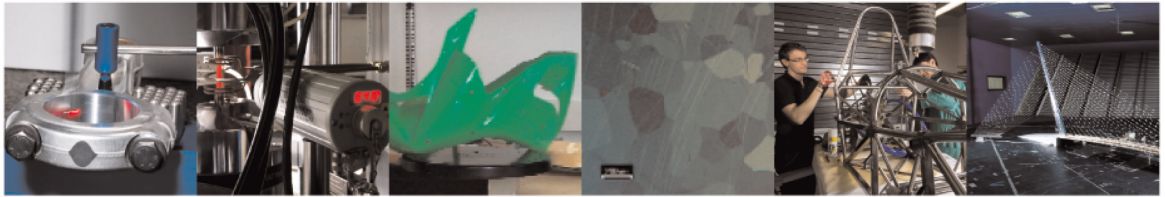POLITECNICO
MILANO 1863

DIPARTIMENTO DI MECCANICA

mecc

Application of semi-active yaw dampers for the improvement of the stability of high-speed rail vehicles: mathematical models and numerical simulation

Wang X.;Liu B.;Di Gialleonardo E.;Kovacic I.;Bruni S.

Application of semi-active yaw dampers for the improvement of the stability of high-speed rail vehicles: mathematical models and numerical simulation

Xu Wang[1], Binbin Liu[2], Egidio Di Gialleonardo[2], Ivo Kovacic[3], and Stefano Bruni[2]

[1] CRRC Qingdao Sifang Co., Ltd., Qingdao, People's Republic of China,
[2] Dipartimento di Meccanica, Politecnico di Milano, Via La Masa 1, Milano 20156, Italy,
[3] Liebherr-Transportation Systems GmbH & Co KG, Liebherrstrasse 1, A-2100 Korneuburg

Binbin Liu (corresponding author)

Department of Mechanical Engineering

POLITECNICO DI MILANO

Via La Masa 1-20156 Milano ITALY

binbin.liu@polimi.it

Application of semi-active yaw dampers for the improvement of the stability of high-speed rail vehicles: mathematical models and numerical simulation

Abstract: The aim of this work is to introduce a new concept for a hydraulic semi-active yaw damper (SAYD) for the improvement of the stability of a high-speed rail vehicle. This concept represents a further elaboration of Secondary Yaw Control but envisages the use of semi-active hydraulic dampers instead of full-active electromechanical dampers, simplifying the design of the system and facilitating the design of a safe and fault tolerant device. Two control algorithms are proposed for the semi-active damper: maximum power point tracking and skyhook with Karnopp approximation. A multi-physics model of the SAYD is introduced and used in co-simulation with a multi-body model of a high-speed vehicle. Using these models, numerical simulations are performed to assess the behaviour of the semi-active damper in terms of improving the running stability of the rail vehicle at very high speed, showing that the use of the SAYD in combination with any of the two control strategies considered allows to improve substantially the stability of the vehicle. The results of experimental investigations performed in the project will be reported in a companion paper.

Keywords: vehicle dynamics, control strategy, semi-active, yaw damper, running stability

1 Introduction

It is well known that the needs of an optimal running stability and curving performance conflict to each other in the design of a rail vehicle [1–4]. In this perspective, secondary yaw dampers are often applied to passenger vehicles, especially for high-speed vehicle, providing additional damping to the bogie modes so that a lower primary yaw stiffness can be used resulting in improved curving performance for the same degree of stability. A proper yaw damper can be developed for this purpose in the design phase of rail vehicles with certain optimisation techniques [5, 6]. However, operational experiences show that the vehicle's stability degrades significantly with the wear evolution of the wheel/rail profiles since the suspension system was originally optimised base on the designed wheel/rail profile combination. Wheel reprofiling is the most straightforward way to solve the problem but implies increased maintenance costs and reduced availability of the vehicle. Furthermore, vehicle stability is also affected by rail profiles and track gauge, which show significant scatter in a real line. As a result, conventional yaw dampers need to be designed for a "worst case" where the combination of a worn wheel profile, restricted track gauge and modified rail profile lead to the highest value of conicity, whilst most of the time the damper will be working in less demanding conditions than the ones assumed in the design.

An alternative solution is to employ an adjustable damper, capable of adapting to the variation of the wheel-rail contact conditions. The adjustable damper can be semi-active or full-active. The concept of active yaw damper has been studied both theoretically and experimentally in labs on roller rigs and in field on real vehicles [2–4,7,8]. Many control strategies are available for the control of the active yaw damper, e.g. modal control, LQG, H∞, skyhook, and fuzzy control where H∞ and LQG are model-based control strategy which generally produces better performances than non-model-based ones while it suffers from unmodelled behaviours and parameters uncertainties. Although many advantages of the active yaw damper in the railway application have been demonstrated through these research works, no commercial application has been reported yet. This is due to the high complexity

and cost implied by this application and also to concerns about the effect of failures in the active suspension.

As a compromise alternative to the full-active damper, the semi-active damper also attracts a lot interest in railway engineering because the semi-active control instead of full-active can make the device simpler and easier to use in cases where reliability, robustness and fault tolerance are the priority. The main difference between the full-active and semi-active dampers is that the former requires external power source which could introduce energy into the system and unstabilize it. The semi-active dampers can be realized by controlling the orifice for traditional hydraulic cylinders or mechanical valves [9,10], or by controlling the fluids for the electrorheological (ER) fluid or magnetorheological (MR) fluid dampers [11,12]. The control strategies introduced above for the full-active suspension are also applicable to the semi-active suspension, whereas specific characteristics of certain adjustable damper (on-off or continuously) must be considered in the development of the control strategy.

It should be noted that past studies available in the literature mainly focus on the application of the semi-active damper to the lateral or vertical suspension system with the aim of improving ride quality [9–12] whilst, to the authors' knowledge, the application of semi-active yaw dampers to railway vehicles has not be reported so far. Still, in the context of mechatronics becoming more and more important in future train generations, a semi-active yaw damper (SAYD) could be an attractive solution offering improved robustness of the vehicle running performance to changes in wheel and track condition, longer life for yaw dampers as for most part of its life the damper would operate under reduced force requirements and also improved ride quality for passengers, as a "stiff" damper leads to increase of noise and vibration transmitted to the car body.

This paper presents some results from a research project jointly carried out by CRRC Qingdao Sifang Co., Ltd, Politecnico di Milano (POLIMI) and Liebherr-Transportation Systems GmbH (LVF). The aim for the new work described in this paper is to introduce a new concept for a hydraulic SAYD for the improvement of the stability of a high-speed rail vehicle and to assess the semi-active hydraulic yaw damper. Compared to previous work published on active yaw dampers e.g. [2], the advantage of this new concept is to use a hydraulic device that can be more easily designed to be fail-safe. On the other hand, the choice to develop a semi-active device rather than a full active one offers advantages in terms of hardware simplification and reduction of costs but shall be verified in terms of the performance offered. The current paper introduces the control strategies for the SAYD and focuses on the assessment of the proposed solution based on Multi-Body Systems (MBS) numerical simulations, while the results of experimental investigations performed in the project will be reported in a companion paper.

This paper is structured as follows. Section 2 describes the numerical model of the Electric Multiple Unit (EMU) vehicle considered in this research and the co-simulation scheme implemented to integrate the SAYD in the vehicle model. Section 3 describes the method used to evaluate the running stability of the EMU vehicle. Section 4 presents the principles of the control strategies considered in this project. Sections 5 and 6 present the results of stability analysis for the EMU vehicle with passive yaw damper configuration and equipped with the SAYD, respectively, for different control strategies. Finally, Section 7 provides some concluding remarks achieved from this research in particular concerning the suitability of the control strategies applied and the effects of the SAYD on the stability of the EMU vehicle.

2 Multi-body system models

The development and verification of the SAYD hardware relied heavily on the use of suitable numerical simulation models, to define the target performance of the damper and to assess its effect on the running behaviour of the vehicle. To these aims an MBS model of the vehicle considered in this research was developed based on actual parameters, see Table 1. The MBS vehicle model consists of a carbody, two bogies with two stages of suspensions and four solid axle wheelsets. The model is made up of rigid bodies with 62 degrees of freedom. There are two yaw dampers arranged in parallel on each side of a bogie. Primary and secondary suspensions are modelled by means of linear and non-linear spring and viscous damping elements. A measure worn wheel profile with a running mileage of 200,000 km called worn S1002CN is used in the simulation to consider a severely degraded contact condition. The contact situation formed between the worn S1002CN and CN60 rail profile with 1:40 cant is shown in Figure 1. Track flexibility is considered by introducing a moving ballast sectional model of the track with lateral and vertical elasticities under each wheelset [13].
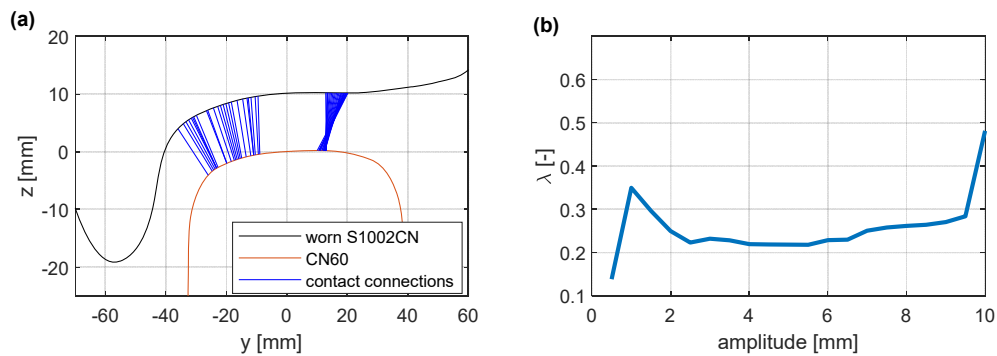

Figure 1 Matching relationship between worn S1002CN and CN60 (a) and equivalent conicity (b)

Table 1 Main parameters of the vehicle model

Wheelset mass [kg]	1550
Bogie frame mass [kg]	2500
Axle load [kN]	150
Primary suspension longitudinal stiffness [MN/m]	100
Primary suspension lateral stiffness [MN/m]	12
Primary suspension vertical stiffness [MN/m]	1.0
Wheelbase [m]	2.5
Rail profile	CN60
Wheel profile	Worn S1002CN

Two different versions of the vehicle model were established, the first one equipped with conventional passive yaw dampers and the second replacing the passive dampers with the new SAYDs. In the following subsections the models of the two dampers are briefly described.

2.1 Passive damper model

The passive yaw damper was modelled using a rheological model made up of two elements: a non-linear viscous damper in series with a linear spring The nonlinear characteristic of the force provided by the passive yaw damper is modelled as a piece-wise function with respect

to velocity as shown in Figure 2. The modelling of the yaw damper is very important in stability assessment of a rail vehicle [14]. A model validation of the passive yaw model was done by comparison to available measurements. The comparisons between the experimental and numerical hysteresis cycles of the yaw damper are reported in Figure 3. These results show the force-displacement hysteresis cycles measured for the dampers in tests performed at different combinations of amplitude and frequency of elongation: 1-2-4 mm amplitude and 1-2-4-6-8-10 Hz frequency. It is observed that the numerical model is able to correctly reproduce the behaviour of the passive damper not only in terms of the maximum force but also of the shape of the hysteresis cycles that are in good agreement to the measurements.
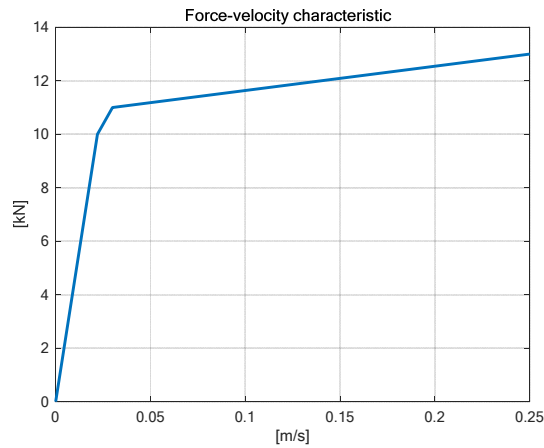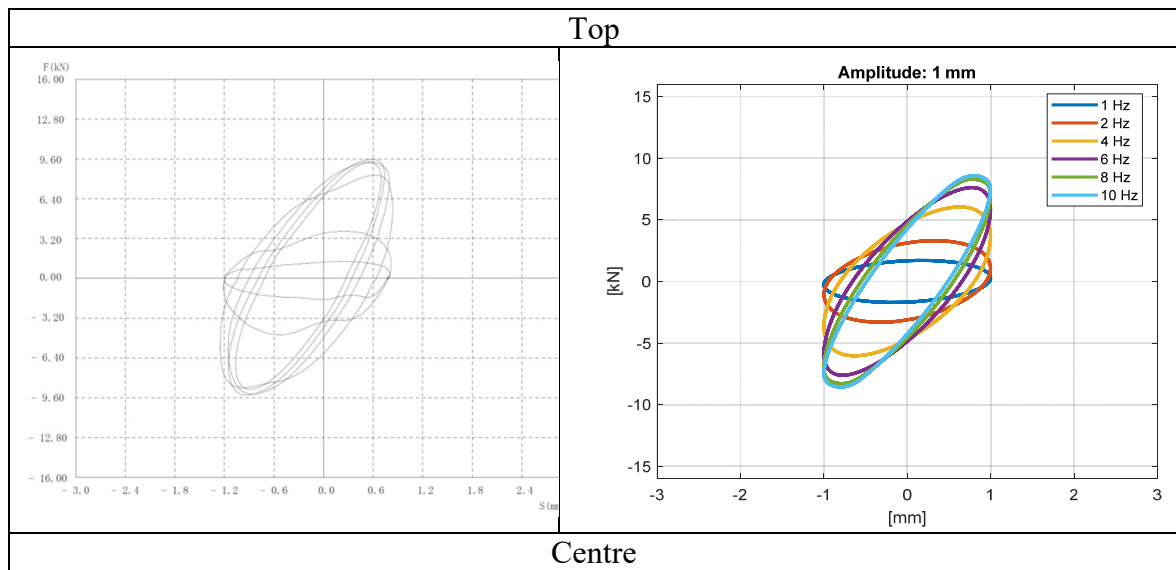

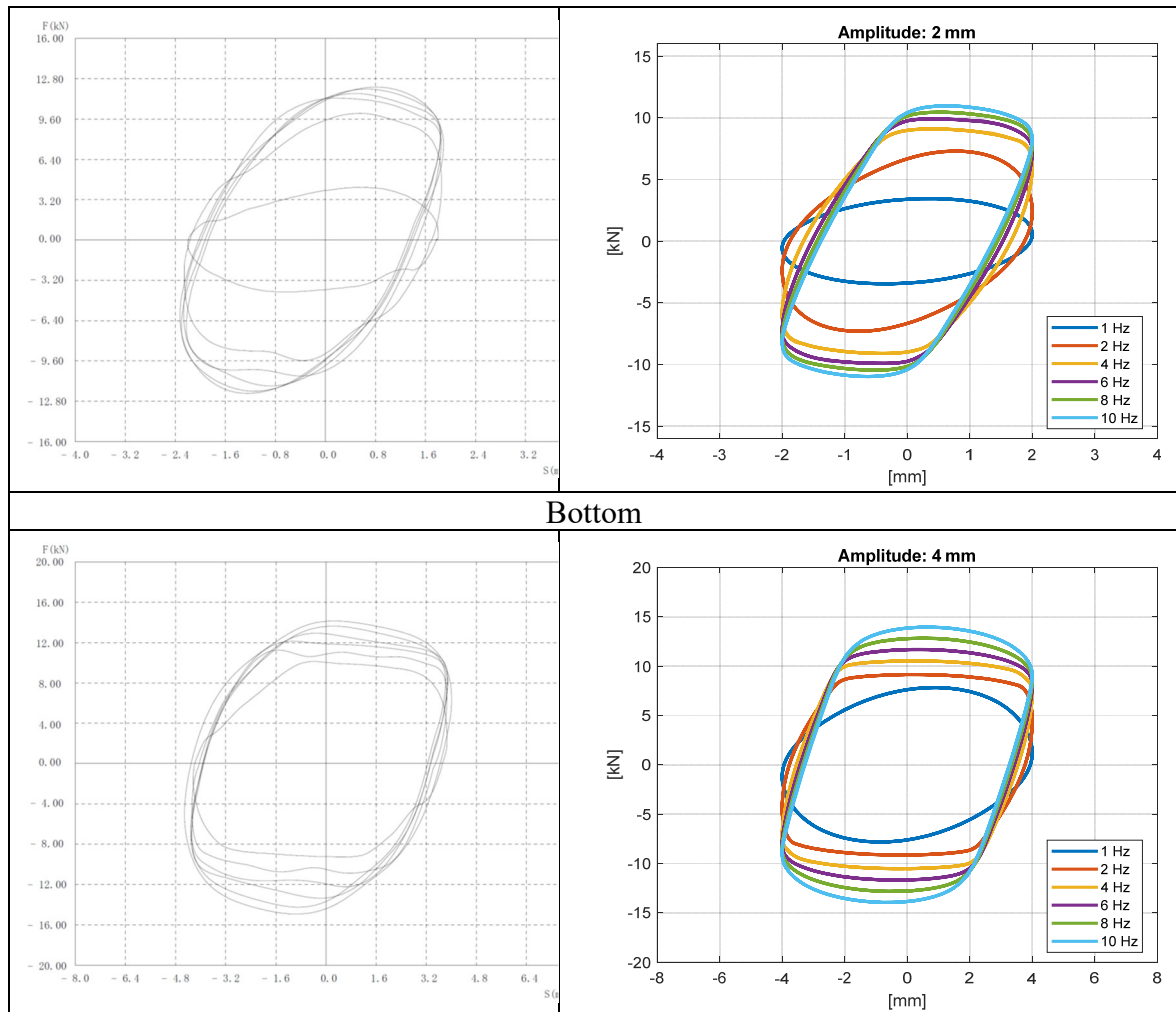**Figure 2 Force-velocity characteristic curve for the yaw damper model.**

Figure 3 The hysteresis cycles of the passive yaw damper: (left) experiment vs. (right) simulation. Top: 1mm amplitude, Centre: 2mm amplitude, Bottom: 4 mm amplitude.

2.2 Semi-active yaw damper model

A numerical model of the SAYD was developed by LVF. The dimensions of the SAYD are the same as the passive one, so it can simply replace the original passive yaw damper of the vehicle with interfaces to receive and send signals for the controller which has been developed based different control strategies of interest. Two SAYDs for each side of the bogie, so eight yaw dampers in total are considered for one single vehicle.

The hydraulic scheme of the SAYD is reported in Figure 4: it essentially consists of the chambers separated by the piston and a tank. The flow between the two chambers is obtained using a flow rectifier circuit made up of an electrically continuously adjustable throttle combined with four check valves. Additional pressure relief and check valves are included into the damper connecting the different parts (chambers, tank) in order to limit the maximum damper force.
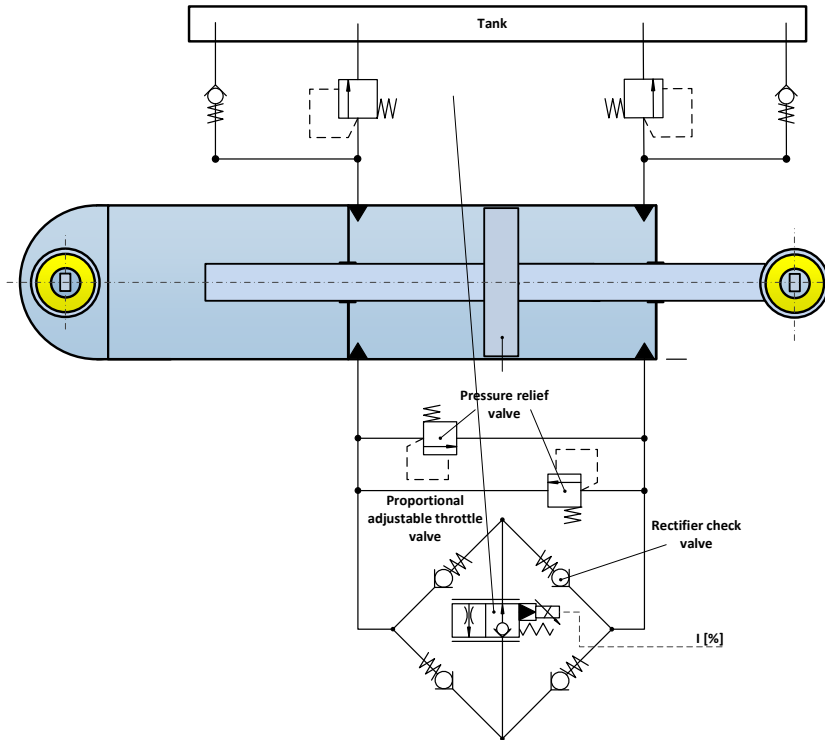
Figure 4 Hydraulic scheme of the semi-active yaw damper.

The simulation model of the SAYD was built considering that an independent movement can be applied to both damper ends. For this purpose, a subdivision in the movement of the piston rod and the damper housing was introduced and the presence of the spherical bearings at the dampers ends was also taken into account, as shown in Figure 5.

The inputs for the mechanical model of the damper are the displacements and the velocities of the connection points between the damper and the bogie (x_1', v_1') and between the damper and the carbody (x_2', v_2'). On the other hand, the outputs of the simulation model, are the forces exchanged through the damper and bogie (F_1) and the damper and the carbody (F_2) in the connection points.
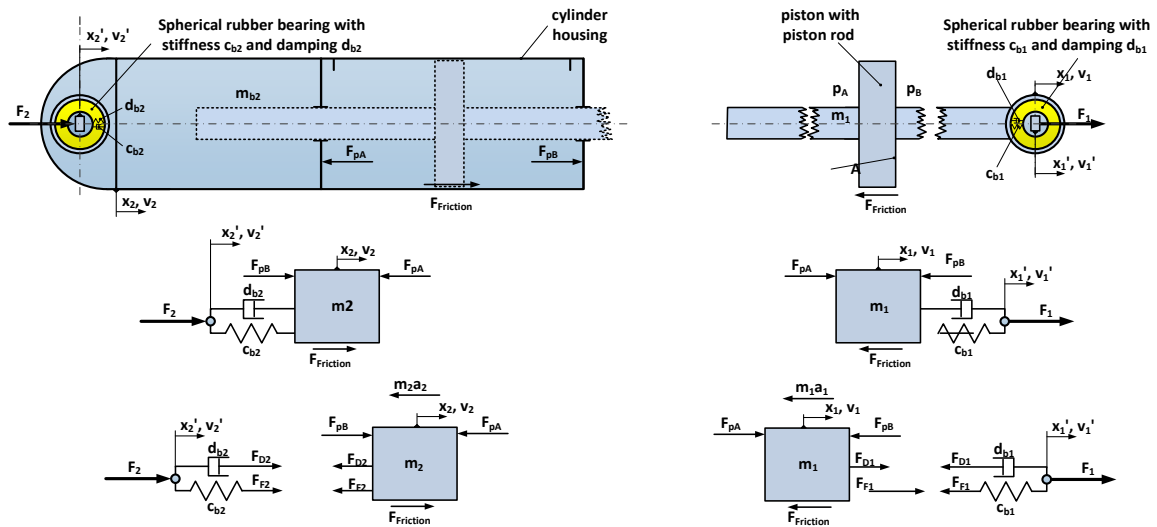

Figure 5 Mechanical scheme of the semi-active yaw damper.

Applying Newton's law to the piston rod, its equation of motion is derived:

$$F_{pA} - F_{pB} + F_{D1} + F_{F1} - F_{Friction} = m_1 \cdot \ddot{x}_1 \tag{1}$$

where:

$$\begin{aligned} F_{D1} &= d_{b1} \cdot (\dot{x}_1 - \dot{x}_1') \\ F_{F1} &= c_{b1} \cdot (x_1 - x_1') \end{aligned} \tag{2}$$

and:

$$F_1 = F_{D1} + F_{F1} \tag{3}$$

On the other hand, considering the motion of the cylinder housing:

$$F_{pB} - F_{pA} - F_{D2} - F_{F2} + F_{Friction} = m_2 \cdot \ddot{x}_2 \tag{4}$$

where:

$$\begin{aligned} F_{D2} &= d_{b2} \cdot (\dot{x}_2 - \dot{x}_2') \\ F_{F2} &= c_{b2} \cdot (x_2 - x_2') \end{aligned} \tag{5}$$

and:

$$-F_{D2} - F_{F2} = F_2 \tag{6}$$

The piston stroke x_{St} results from the position x_1 and x_2:

$$\ddot{x}_{St} = \ddot{x}_1 - \ddot{x}_2$$

$$\dot{x}_{St} = (\dot{x}_1 - \dot{x}_2) + \underbrace{\dot{x}_{St,0}}_{\dot{x}_{1,0} - \dot{x}_{2,0}} \tag{7}$$

$$x_{St} = (x_1 - x_2) + \underbrace{x_{St,0}}_{x_{1,0} - x_{2,0}}$$

With the initial condition $x_{St,0} = x_{1,0} - x_{2,0} = L_0$ the damper stroke results as follows:

$$x_{St} = (x_1 - x_2) - L_0 \tag{8}$$

The equation of motion for the damper stroke can be derived:

$$\ddot{x}_{St} = \frac{1}{m_1}\left(\underbrace{F_{pA} - F_{pB}}_{+F_p} + \underbrace{F_{D1} + F_{F1}}_{+F_1} - F_{Friction} \right) - \frac{1}{m_2}\left(\underbrace{F_{pB} - F_{pA}}_{-F_p} \underbrace{-F_{D2} - F_{F2}}_{+F_2} + F_{Friction} \right) \tag{9}$$

$$\ddot{x}_{St} = F_p \left(\frac{1}{m_1} + \frac{1}{m_2} \right) - F_{Friction}\left(\frac{1}{m_1} + \frac{1}{m_2} \right) + \frac{1}{m_1} F_1 - \frac{1}{m_2} F_2 \tag{10}$$

Thus, the mechanical model of the damper has two degrees of freedom which can be chosen among the variables x_1, x_2 and x_{St}. Since the friction force is associated to the relative motion between the piston and the cylinder, described by the variable x_{st}, the damper stroke x_{st} and the displacement of the piston x_1 are used as independent variables.

As far as the friction force is considered, it is modelled using a typical Coulomb approach where F_C.represents the stiction force and F_S the sliding friction.

Thus, the friction force can be defined as:

$$F_{Friction} = \begin{cases} F_{ext} & \dot{x}_{St} = 0 & \& & |F_{ext}| < F_C \\ F_C \cdot \text{sign}(F_{ext}) & \dot{x}_{St} = 0 & \& & |F_{ext}| \geq F_C \\ F_S \cdot \text{sign}(\dot{x}_{St}) & \dot{x}_{St} \neq 0 \end{cases} \tag{11}$$

Reworking equation (10), the following equation relating the damper stroke x_{st} to the forces acting on the damper:

$$\frac{m_1 \cdot m_2}{m_1 + m_2} \ddot{x}_{St} = -F_{Friction} + F_p + \underbrace{\frac{m_2}{m_1 + m_2} F_1 - \frac{m_1}{m_1 + m_2} F_2}_{F_{ext}} \tag{12}$$

The terms F_p, F_{pA} and F_{pB} inside the equations represent the forces acting on the damper due the pressures of the two piston chambers p_A and p_B which can be expressed via a pressure build up equation.
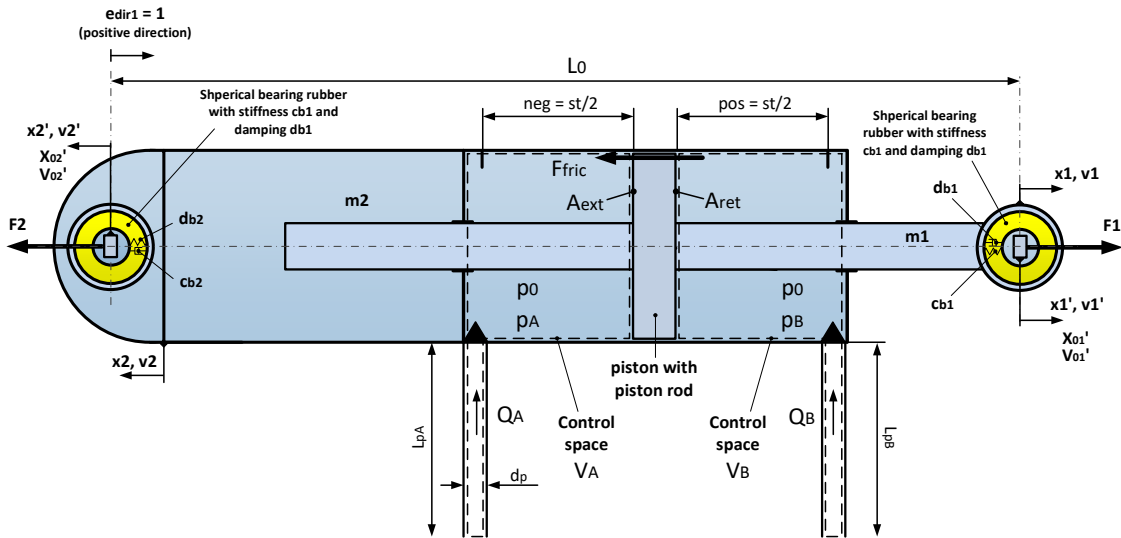

Figure 6 SAYD model configuration.

The pressure build-up equation is derived from the continuity relationship:

$$\dot{M} = \frac{dM}{dt} = Q \cdot \rho \tag{13}$$

$$\frac{dM}{dt} = \frac{d(\rho V)}{dt} = \dot{\rho} V + \rho \dot{V} \tag{14}$$

and the compressibility law

$$\rho = \rho_0 \left(1 + \frac{p - p_0}{E}\right) \tag{15}$$

where the parameter E defines the bulk modulus of the oil.

$$\rho_0 \frac{\dot{p}}{E}(V_0 + A\,x_{St}) + \rho_0 \underbrace{\left(1 + \underbrace{\frac{p}{E}}_{p \ll E}\right)}_{\approx 1} A\,\dot{x}_{St} = Q \cdot \rho \tag{16}$$

$$\dot{p} = \frac{E}{V_0 + A\,x_{St}}(-A\,\dot{x}_{st} + Q) \tag{17}$$

The resulting general pressure build-up equation is used to describe the chamber pressures p_A and p_B of the SAYD. Taking into account the geometries of the control spaces from Figure 6, the pressure build-up equations for the pressures p_A and p_B result as follows:

$$\dot{p}_A = \frac{E}{V_{A0} + A\,x_{St}}(-A\,\dot{x}_{St} + Q_A) \tag{18}$$

$$\dot{p}_B = \frac{E}{V_{B0} - A\,x_{St}}(A\,\dot{x}_{St} + Q_B) \tag{19}$$

with:

$$V_{A0} = st/2 \cdot A + L_{pA} \cdot \frac{d_p^2 \cdot \pi}{4} \tag{20}$$

$$V_{B0} = st/2 \cdot A + L_{pB} \cdot \frac{d_p^2 \cdot \pi}{4} \tag{21}$$

Q_A and Q_B are the flow rates entering the control spaces, accounting for the effect of the proportional adjustable throttle valve together with the rectifier circuit and all the others check and pressure relief valves shown in Figure 4.

The flow through the proportional adjustable throttle is obtained by means of a 2D-lookup table. The opening of the proportionally adjustable valve depends on the coil current (which is the control variable) and consequently the pressure-flow characteristics for different current values were stored in a 2D lookup table, resulting in a characteristic curve field which describes the quasi-static pressure and flow characteristic as a function of the different current values.

On the other hand, the flow through a fully open pressure relief valve is described by the following flow equation:

$$Q = Q_N \cdot \sqrt{\frac{\Delta p}{\Delta p_N}} \tag{22}$$

where Q_N is the nominal valve flow rate and Δp_N is the nominal pressure drop of the pressure relief valve when the valve is fully open. For an incompletely opened pressure relief valve the following relationship for the flow through the valve is used:

$$Q = Q_N \cdot \sqrt{\frac{p_s}{\Delta p_N}} \cdot \frac{(\Delta p - p_o)}{p_s - p_o} \tag{23}$$

where p_o is the effective pressure difference across the pressure relief valve at which the valve begins to open and p_S is the effective pressure difference at which the pressure relief valve is fully open. Taking the pressure conditions into account, the model for the pressure relief valve is described as follows:

$$
Q = \begin{cases}
0 & \Delta p < p_o \\
Q_N \cdot \sqrt{\dfrac{p_S}{\Delta p_N}} \cdot \dfrac{(\Delta p - p_o)}{p_S - p_o} & p_o \leq \Delta p \leq p_S \\
Q_N \cdot \sqrt{\dfrac{\Delta p}{\Delta p_N}} & p_S < \Delta p
\end{cases} \tag{24}
$$

The same method was used to model the check valves, whereby the pressure ratios (opening pressure p_o and pressure with fully opened valve p_S) as well as the nominal flows and pressure losses of the respective components were taken from the respective component data sheets and stored in the corresponding check valve or pressure relief valve model.

The SAYD model and its controller were incorporated into the MBS vehicle model by means of a co-simulation approach, as schematically shown in Figure 7.

Summing up, the SAYD model is a dynamical model having 6 states (4 mechanical states and 2 hydraulic ones).

The inputs of the SAYD model are as follows:

a)   Valve current which is the signal driving the adjustable throttle in the damper, resulting in the change of the damping ratio. This input is defined according to different control strategies as detailed in Section 4 of this paper;
b)   Displacements and velocities of the connection point of the damper on the bogie and the carbody. These inputs of the SAYD are extracted from the MBS model of the vehicle.

The outputs of the SAYD model are:

a)   The damper force which is fed back in the MBS model of the vehicle;
b)   The pressure in the two chambers of the damper. This signal is used in the MPPT control strategy, see Section 4.
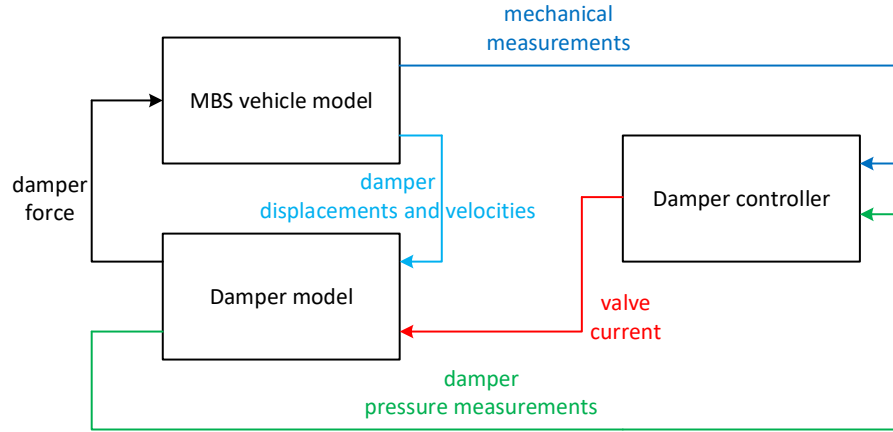
Figure 7 Co-simulation approach for the simulation of the dynamics of the vehicle equipped with SAYD.

3 Procedure for the assessment of the stability of the vehicle

The behaviour of the vehicle in straight track was investigated in terms of its non-linear stability, i.e. the occurrence of periodic oscillations as the result of self-excited vibrations caused by wheel-rail contact forces. Different methods can be used to evaluate the non-linear critical speed of an MBS simulation, and a review is provided in [25]. The method used in this work replicates the procedure prescribed by the European standard EN14363 [15] for the assessment of vehicle stability based on line tests.

Simulations are performed considering the vehicle running at constant speed in straight track, subjected to random excitation caused by track irregularities. From these simulations, the raw time histories of different assessment quantities are extracted, namely:

- the track shift forces (sum of guiding forces on the two wheels of the same axle) for the four wheelsets of the vehicle. This assessment quantity is the one considered by the 'complete measuring method' according to standard EN14363;
- the lateral acceleration of the bogie frame measured above the axleboxes of the four wheelsets. This assessment quantity is the one considered by the 'simplified measuring method' according to standard EN14363.

The signal processing is the same for all the assessment quantities and consists of the following steps:

1) a pass-band filter is applied on the signal with pass band $f_0 \pm 2$ Hz, f_0 being the dominant frequency, defined as the frequency of the harmonic component in the signal having largest amplitude. To reduce the fluctuations in the value of f_0 which are caused by the randomness of the signal, the FFT algorithm is applied to relatively short segments of the signal, corresponding to a distance run of 500 m, and the different spectra obtained are averaged;
2) the sliding RMS of the signal is computed over a 100 m window length updated in 10 m steps;
3) the maximum of the sliding RMS is compared to a limit value defined below.

For the track shift forces, the limit value is defined as 50% of the Prud'homme limit:

$$Y_{lim} = \frac{1}{2}\left(10 + \frac{P}{3}\right) \tag{25}$$

with P the axle load and both P and ΣY_{lim} defined in kN.

For the lateral acceleration of the bogie frame the limit value is defined as:

$$\ddot{y}_{lim}^+ = \frac{1}{2}\left(12 - \frac{m_b}{5}\right) \tag{26}$$

with $\ddot{y}_{lim}^+$ expressed in m/s^2 and being m_b the mass of the bogie in tons.

The above described procedure is repeated increasing in steps the speed of the vehicle until the limit value is exceeded for any of the assessment quantities.

Figure 8 shows an example of application of the signal processing procedure for the vehicle with conventional passive dampers and with new wheel profiles. The lateral acceleration of the bogie frame is considered as the assessment quantity. The upper plot shows the results of the signal processing procedure performed for the speed of 280 km/h: the solid line represents the filtered time history, the line with crosses represents the sliding RMS and the dashed horizontal line represents the limit value.

In this running condition the vehicle shows a stable running behaviour with the sliding RMS values well below the limit. The lower plot shows the trend with speed of the assessment quantity (solid line, the circles represent the speed values at which simulations were run) and the limit value (horizontal dashed line). Considering linear interpolation, the non-linear critical speed of the vehicle for this configuration is estimated to be slightly higher than 370 km/h. The dominant frequency of the signal (not shown for the sake of brevity) is found to be approximately 4 Hz when the vehicle runs at the critical speed.
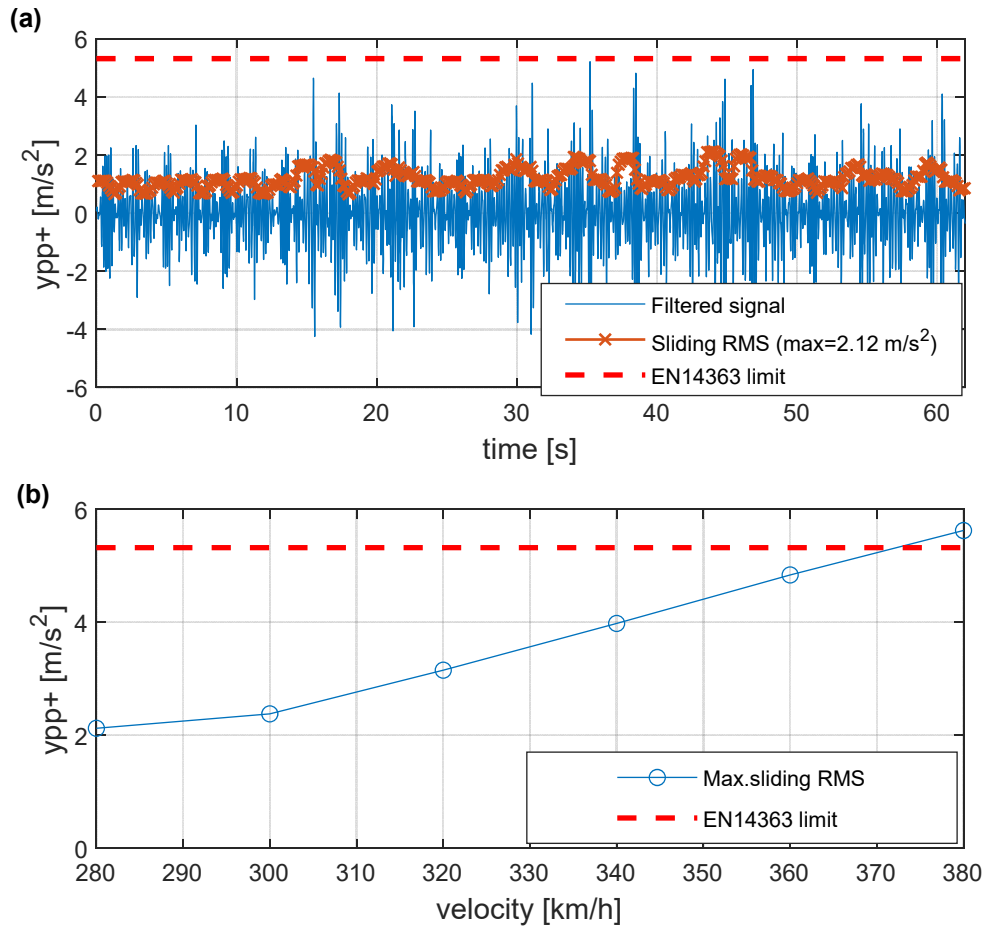
Figure 8 Time history of the pass-band filtered lateral acceleration signal (blue line), sliding RMS (red line with crosses), EN14363 limit (dashed line)(a) and maximum sliding RMS as a function of velocity (b).

4 Control strategies

A large number of attempts in applying control system design approaches to railway suspension systems are present in literature [16]. Many papers have been concerned with active suspensions, since they permit to obtain better performances while the control synthesis does not require to handle dissipative properties of the semi-active device. In general, the semi-active suspension control literature is also quite large [17], and an important number of control strategies exist for such a system, but a limited number of applications are referred to railway vehicles.

Among different control approaches, varying from classical (typically skyhook) to modern ones (optimal controllers, model predictive controllers,…) the choice was restricted to non-model based approaches, so to have a simple solution avoiding also the degradation of the controller performances due to model uncertainties.

With this regards, two control strategies suitable for control of semi-active dampers are considered in this study:

1) Maximum Power Point Tracking (MPPT) [18]: this is a heuristic strategy which tracks the optimum working condition for the damper.

2)   skyhook strategy [19]. In this strategy the semi-active damper is operated to mimic the behaviour of a virtual viscous damper connecting the bogie frame to a virtual fixed point, thus maximising energy dissipation for the hunting motion of the bogie.

Some additional details about the two control strategies are provided below.

4.1   MPPT control strategy

The MPPT control strategy was developed in origin to adjust the controller variables with the aim of maximizing the power generated in a production plant [20,21]. It is a simple algorithm of minimum search that can be used to track the maximum or minimum of a function of the system's state.

In its original version, it is not applicable to the problem under analysis, therefore the control algorithm is modified in order to be applied also to a purely mechanical system: the problem is formulated as the minimisation of a cost function J considering the vehicle's stability performance and the force required from the semi-active damper. The cost function is defined as:

$$J = k_{\ddot{y}} \left(\frac{\psi_{\ddot{y}}}{\ddot{y}_{lim}^{+}} \right)^2 + k_F \left(\frac{\psi_F}{F_{Max}} \right)^2 \tag{27}$$

where $\psi_{\ddot{y}}$ is the RMS of the bogie frame lateral acceleration, measured by an accelerometer mounted on the bogie frame and filtered according to the prescriptions of the EN14363 standard (pass-band filter with pass band $f_0 \pm 2$ Hz, see Section 3), ψ_F is the RMS of the hydraulic force generated by the damper, $\ddot{y}_{lim}^{+}$ is the limit value for the lateral acceleration of the bogie frame defined by equation (26), F_{Max} is set to 12 kN and finally $k_{\ddot{y}}$ and k_F are two non-dimensional weighting factors. The force generated by the damper is estimated from the pressures measured in the two chambers p_1 and p_2 as:

$$F = A_1 p_1 - A_2 p_2 \tag{28}$$

with A_1 and A_2 the area of the piston in the two chambers.

The minimum value of the cost function J is representing the damper's optimal working condition and different trade-offs between improving vehicle stability (low RMS of lateral bogie frame acceleration) and reducing the control force (low value of ψ_F) can be obtained by using different combinations of weights. Functional J is evaluated at discrete time intervals of 1 s, referred here as 'steps'. The new value of the valve opening command V^{n+1} for step $n+1$ is defined starting from the value of the command at the previous step V^n based on the difference between the value of the cost function at steps n and $n+1$, J^n and J^{n+1} respectively, according to the following equation:

$$V^{n+1} = V^n - k_J \left(\frac{J^{n+1} - J^n}{\max (J^n, J^{n+1})} \right) \tag{29}$$

where k_J is a gain constant.

In order to improve the promptness of the MPPT control strategy in reacting to changed conditions in the stability of the vehicle, the following rule is added to the control strategy:

$$V^{n+1} = V^n - \Delta V \qquad \text{if } RMS(\ddot{x}_{bogie}) > \ddot{x}_{th,max} \qquad (30)$$

where $\ddot{x}_{th,max}$ is an upper threshold value defined for the bogie frame acceleration. In this way, the control strategy immediately starts to close the valve once a large RMS value is detected for the bogie frame acceleration.

A second condition is applied when the RMS of the acceleration is below a lower threshold corresponding to a condition very far from instability:

$$V^{n+1} = V^n + \Delta V \qquad \text{if } RMS(\ddot{x}_{bogie}) < \ddot{x}_{th,min} \qquad (31)$$

where $\ddot{x}_{th,min}$ is the lower threshold for bogie frame acceleration. In this latter case, the control strategy is forced to re-open the valve as soon as the acceleration of the bogie becomes sufficiently low, so that the promptness of the controlled damper to reduce the force transmitted is improved.

The MPPT control strategy was implemented with two sets of weights in the cost function as follows:

- **MPPT1** only weights performance. This strategy requires one accelerometer to measure the lateral acceleration of the bogie frame.
- **MPPT2** weights the performance and the force generated in the damper. This strategy requires one accelerometer (same as for strategy MPPT1) and two pressure pick-ups in the two chambers of the SAYD.

4.2 Skyhook strategy

The skyhook strategy generates a damping force proportional to the absolute longitudinal velocity of the bogie frame $\dot{x}$, thus emulating the effect of a damper connecting the bogie frame to a virtual fixed point:

$$F_{Ref} = -c_{sky}\dot{x} \qquad (32)$$

Because in this project a semi-active damper is used instead of a full-active one, the skyhook control force can only be approximated. The actual force F_{YD} generated by the damper is:

$$F_{YD} = c_{YD}\Delta\dot{L} \qquad (33)$$

where c_{YD} is the damping coefficient of the yaw damper, which can be tuned in the semi-active damper, and $\Delta\dot{L}$ is the speed of elongation of the damper.

Prescribing the actual force F_{YD} generated by the damper to be the desired force F_{sky} the following desired value of the variable damping coefficient c_{YD} is obtained:

$$c_{YD} = c_{sky}\frac{\dot{x}}{\Delta\dot{L}} \qquad (34)$$

However, the damping coefficient realised by the semi-active damper c_{YD} shall be within the lower and upper limits corresponding to the design of the damper:

$$c_{min} \leq c_{YD} \leq c_{max} \tag{35}$$

hence, the saturated ideal damping coefficient to be generated by the semi-active damper is:

$$c_{YD} = \begin{cases} min\left[c_{sky}\dfrac{\dot{x}}{\Delta\dot{L}}, c_{max}\right], & \dot{x}\Delta\dot{L} \geq 0 \\ c_{min}, & \dot{x}\Delta\dot{L} < 0 \end{cases} \tag{36}$$

In the case of a semi-active yaw damper, the desired damping coefficient c_{sky} should be as high as possible, hence it is set to the maximum damping that can be realised by the damper: $c_{sky} = c_{max}$. It follows that equation (36) becomes:

$$c_{YD} = \begin{cases} min\left[c_{max}\dfrac{\dot{x}}{\Delta\dot{L}}, c_{max}\right], & \dot{x}\Delta\dot{L} \geq 0 \\ c_{min}, & \dot{x}\Delta\dot{L} < 0 \end{cases} \tag{37}$$

Equation (37) provides the value of the desired damping in the continuous skyhook strategy. Alternatively, to simplify the switching of the damper an on-off strategy can be used. In this case, the damping coefficient is simply switched between the highest and lowest possible values according to:

$$c_{YD} = \begin{cases} c_{max}, & \dot{x}\Delta\dot{L} \geq 0 \\ c_{min}, & \dot{x}\Delta\dot{L} < 0 \end{cases} \tag{38}$$

In both cases of the continuous and on-off skyhook control strategy, two sensors are required: one accelerometer to measure the longitudinal acceleration of the bogie frame to be which is integrated to derive the absolute longitudinal velocity of the bogie frame $\dot{x}$ and one displacement transducer, incorporated in the SAYD hardware, to measure the elongation of the damper ΔL, from which the speed of elongation of the damper $\Delta\dot{L}$ is obtained by means of numerical derivation A schematic presentation of the skyhook control strategy is provided in Figure 9.
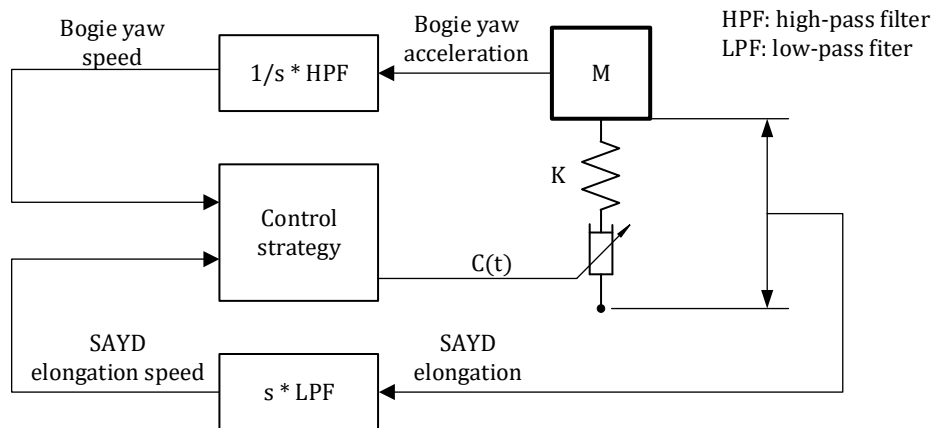

Figure 9 Scheme of skyhook control strategy

5 Simulation results

In this section the procedure described in Section 3 is applied in order to assess the effectiveness of using a SAYD in place of a passive one and to compare the control strategies developed in this work.

5.1 EMU vehicle with passive yaw damper

Firstly, the procedure to evaluate the non-linear stability of the vehicle is applied to the baseline case, i.e. the vehicle equipped with passive yaw dampers.

Figure 10 summarises the results of the analysis performed according to this procedure. The upper subplot shows only the trend with speed of the dominant frequency obtained from the process of the bogie acceleration since a very similar trend can be obtained if the force signal is considered while central and bottom subplots show the trend with speed of the maximum of the sliding RMS of the track shift force and of bogie acceleration respectively. Track shift forces are shown for all four wheelsets in the vehicle (labelled as WS1 to WS4 with WS1 the leading wheelset of the front bogie) and lateral accelerations are shown for four measuring points on the bogie frames above each wheelset, also labelled as WS1 to WS4.

The stability analysis is performed in the speed range from 320 to 445 km/h. At the lowest speed considered, 320 km/h, all assessment quantities are below the corresponding limit, showing a stable behaviour of the vehicle. At this speed, the dominant frequency in the signals is different for the four wheelsets, as the motion of the bogie is due partly to the hunting motion and partly to the excitation from random track irregularities. Because at this speed the contribution due to the hunting motion is not fully dominant, a scatter is observed in the evaluation of the dominant frequency.

The trend of the assessment quantities is monotonically increasing with the speed of the vehicle and the threshold on lateral accelerations is exceeded in all simulation cases run at speed equal to 350 km/h or higher. The maximum sliding RMS of track shift forces is significantly higher for the trailing wheelsets of the two bogies compared to the leading wheelsets. A justification for the higher value of the track shift force on the trailing axle of each bogie is provided in [26]. The lowest speed at which the threshold value is exceeded for the assessment quantities derived from track shift forces is 370 km/h. Therefore, the non-linear critical speed estimated based on the sliding RMS of bogie accelerations (simplified measuring method, according to the terminology of EN14363) is lower than the one estimated based on track shift forces (normal measuring method according to EN14363). This is consistent to what was found in literature and reported in [25]. Applying linear interpolation to the trend of the maximum sliding RMS of the lateral acceleration, a critical speed of approximately 330 km/h is obtained for the passive vehicle. At speed 350 km/h or higher, the dominant frequency is the same for all assessment quantities, showing the actual dominance of the hunting cycle in the lateral motion of the vehicle. In this speed range, the dominant frequency is increasing with vehicle speed, which is consistent with the mechanism of hunting motion.
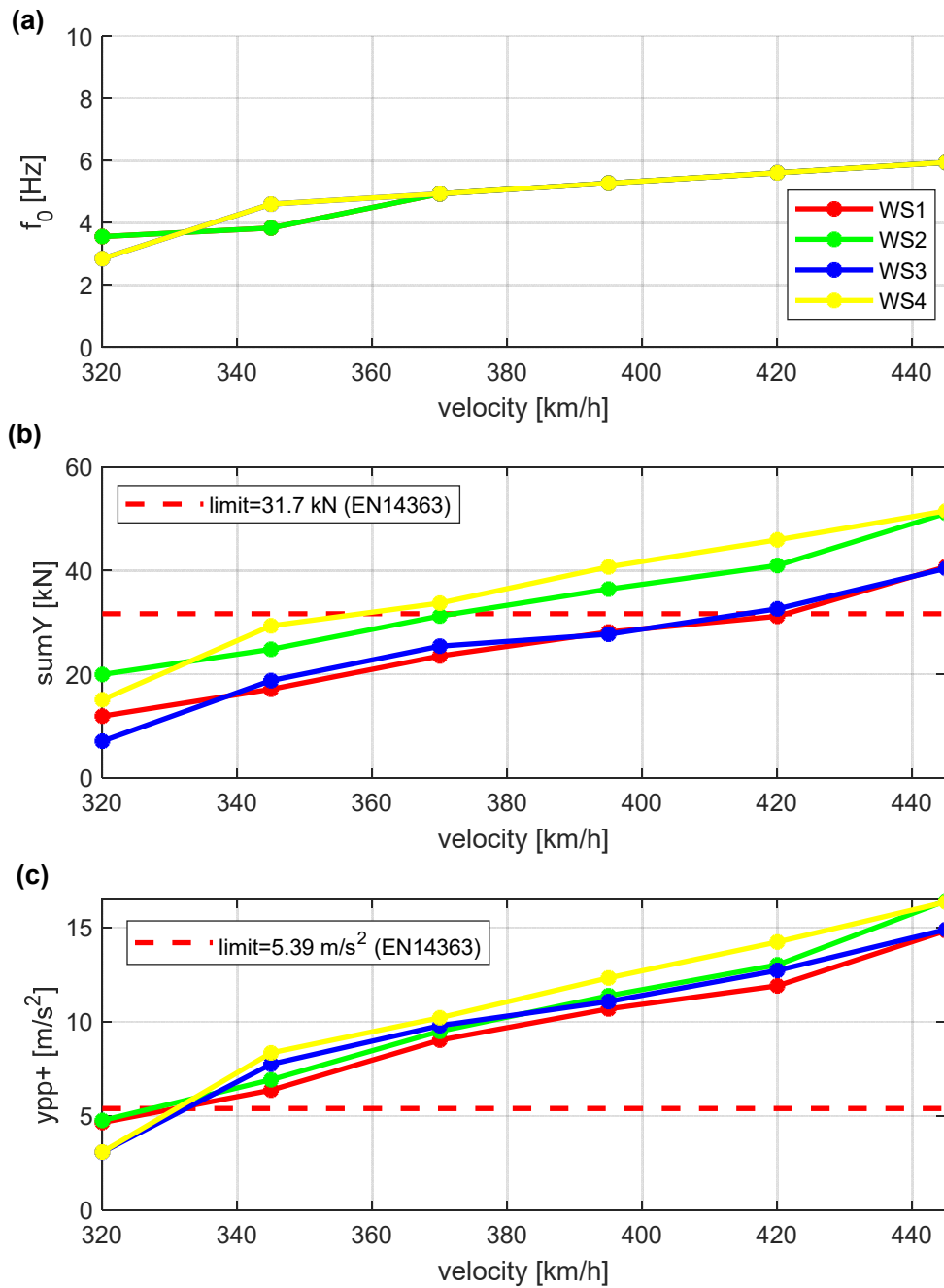
Figure 10 Dominant frequency(a), RMS of the track shift force (b) and of the acceleration of bogie frame (c) as function of vehicle velocity for the passive vehicle

5.2 EMU vehicle with semi-active yaw damper

In the next phase of the work, the passive yaw dampers of the EMU vehicle are replaced by SAYDs and the co-simulation model described in Section 2 is used to investigate the influence of the semi-active yaw damper on the stability of the EMU vehicle considering the control strategies described in Section 4 of this paper. The simulation results are presented in the following subsections.

5.2.1 EMU vehicle with SAYD controlled by MPPT1 strategy

As described in Section 4, the MPPT1 version of the general MPPT control strategy only aims at improving the performance of the vehicle in terms of reducing the RMS of the pass-band filtered lateral acceleration measured at the bogie frame.

As already shown for the vehicle equipped with passive dampers, the simplified measuring method (i.e. the evaluation of the nonlinear critical speed based on the lateral acceleration of the bogie frame) is more conservative with respect to the normal measuring method. Thus, for the sake of brevity, only the results showing the trend with speed of the dominant frequency and filtered RMS of the lateral bogie frame acceleration are presented in Figure 11: from these results it is observed that in this configuration the vehicle is highly stable in the entire range of speeds considered in the analysis up to 400 km/h with low values of the sliding RMS of the lateral bogie frame acceleration, showing a very large stability margin even at the highest speed considered. The trend with vehicle speed of the dominant frequency is irregular, because the excitation caused by random track irregularities prevails over the effect of hunting motion, so that there is actually no dominant harmonic term in the spectrum of the lateral acceleration and hence the dominant frequency defined according to the method described in Section 3 varies randomly between 2 and 10 Hz.
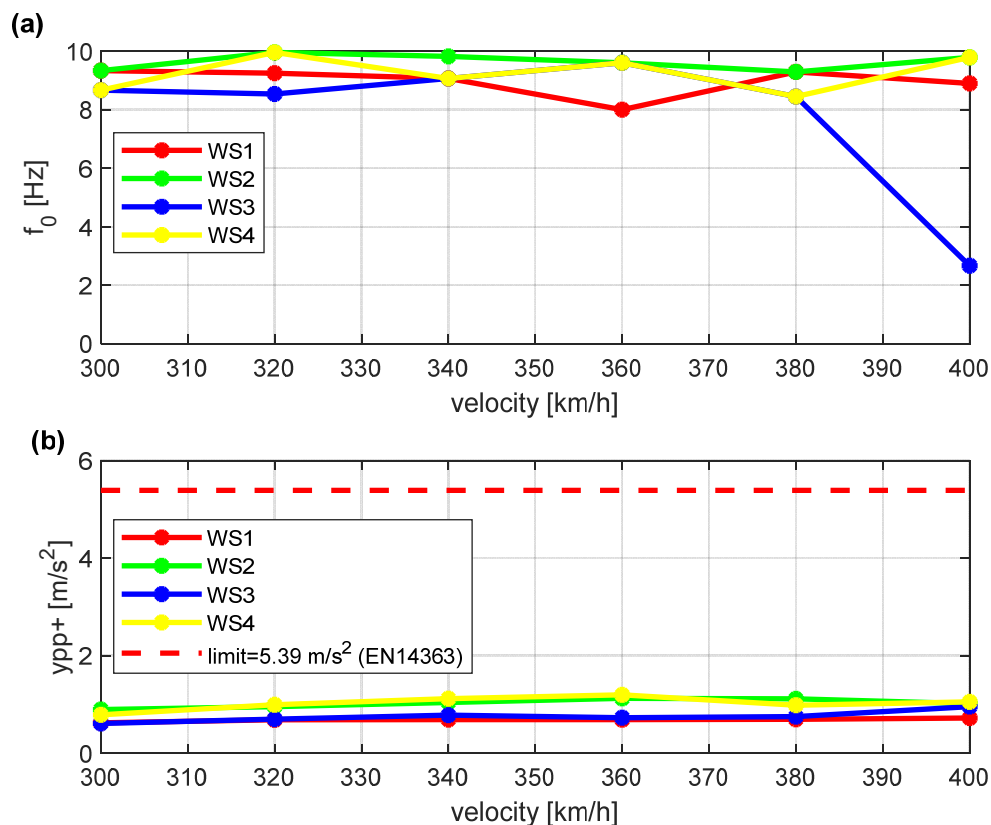

Figure 11 Dominant frequency (a) and RMS of the acceleration of bogie frame (b) as function of vehicle velocity with MPPT1 control

Figure 12 shows the time history of the valve current (upper subplot) and damper force (lower subplot) for the simulation performed at 400 km/h, i.e. the maximum speed

considered in the analysis. The valve current is the command to the SAYD controlling the opening of the controlled valve: for current 0% the valve is fully closed whilst for valve current 100% the valve is fully open. For the sake of brevity, only the command for the rear bogie and the damper force on one damper of the rear bogie are shown, the time histories of valve command of the other bogie and of the force in other dampers show similar trends.

Two cases are presented considering the valve command starting at fully closed (V=0%) and fully open (V=100%) conditions, respectively. For the first case, the valve current values are in the 5-10% range, showing that the damper operates close to the fully closed position. This is due to the fact that the SAYDs are required to provide a strong damping effect to ensure the stability of the vehicle at the very high speed considered, but is also the consequence of the control strategy adopted, which is entirely aimed at maximising vehicle stability, with no consideration of reducing the damping force. In case the command starts at V=100% the command is rapidly decreased so that in the first 5 seconds of the simulation gets to approximately closed position, then follows the same trend of the first case. In the lower subplot only the time history of the damper force for the case starting at V=0% is shown but the result for the case starting at V=100% is very similar.
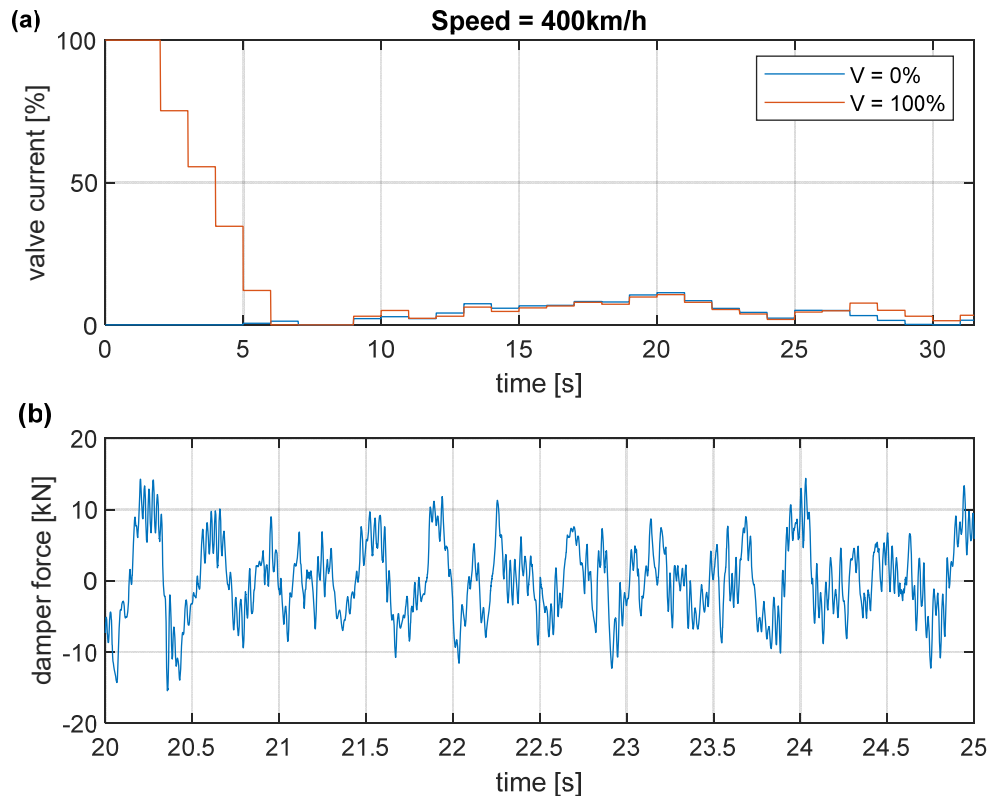

Figure 12 Time history of the valve current (a) and the force of SAYD (b) at speed 400km/h with MPPT1 control. Top: valve current (command to the controlled valve). bottom: damper force.

5.2.2   EMU vehicle with SAYD controlled by MPPT2 strategy

This version of the MPPT aims at a compromise between improving the performance of the vehicle in terms of reducing the RMS of the pass-band filtered lateral acceleration measured at the bogie frame and minimising the damper force, that is related to the transmission of vibrations towards the carbody.

Figure 13 shows the trend with speed of the dominant frequency and filtered RMS of the lateral bogie frame acceleration. In terms of vehicle stability, no major difference is found compared to the previous case with the MPPT1 version of the controller: the vehicle is stable up to 400 km/h with low values of the sliding RMS of bogie accelerations.
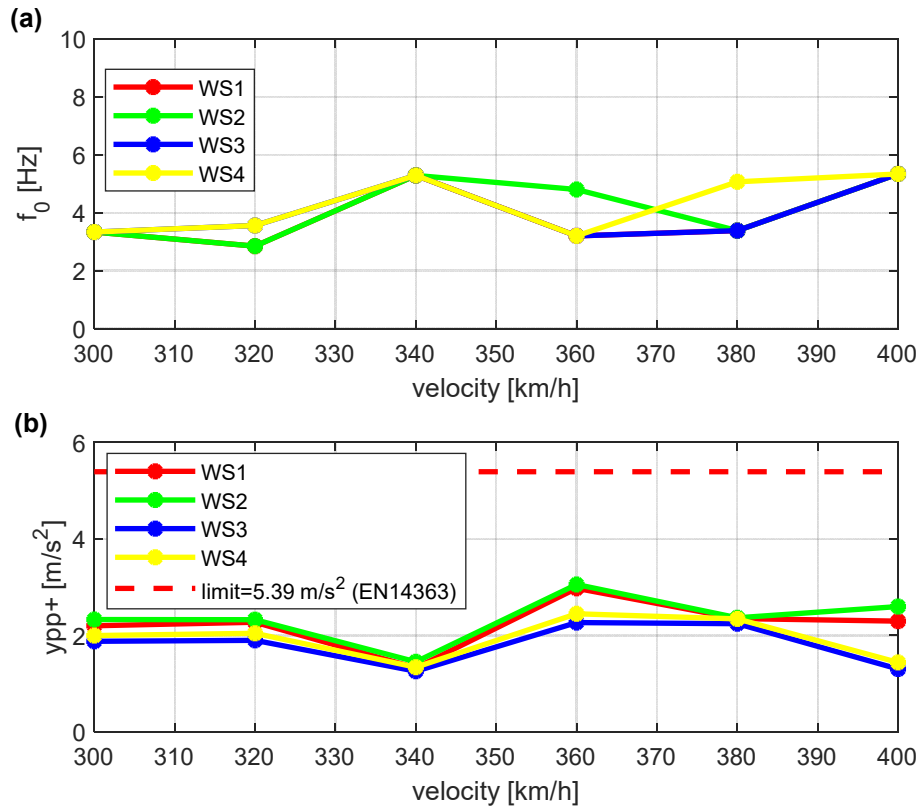

Figure 13 Dominant frequency (a) and RMS of the acceleration of bogie frame (b) as function of vehicle velocity with MPPT2 control.
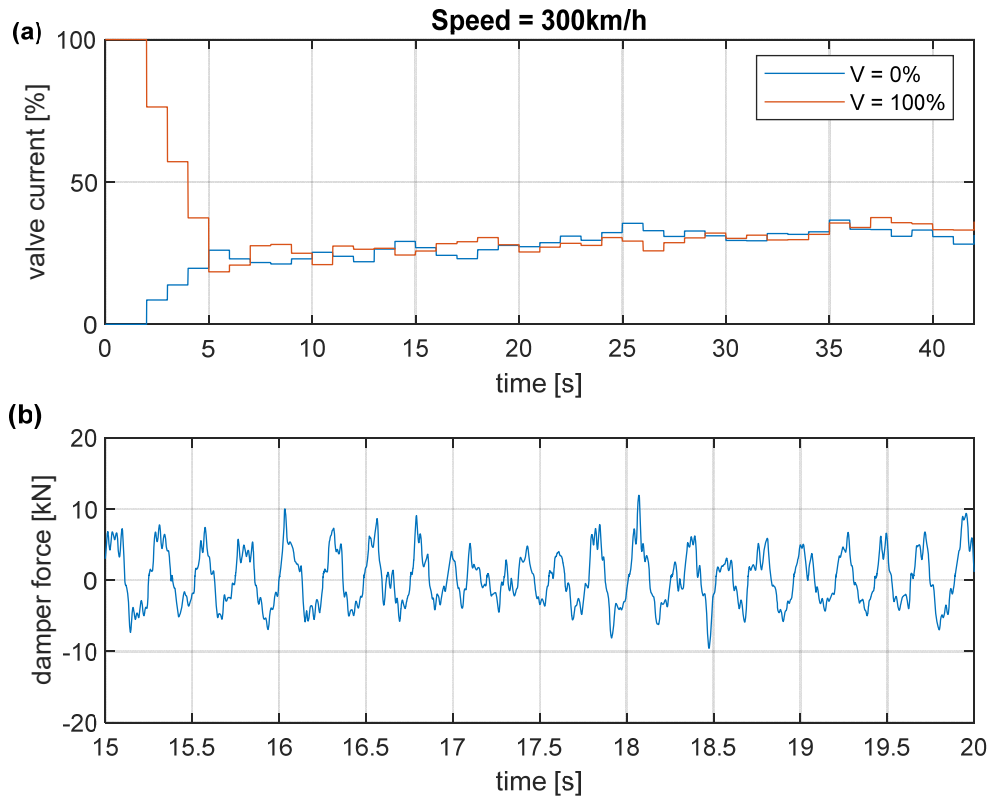
Figure 14 Time history of the valve current (a) and the force of SAYD (b) at speed 300km/h with MPPT2 control. Top: valve current (command to the controlled valve). bottom: damper force.

Figure 14 shows the time history of the valve current for the simulation performed at 300 km/h. Deliberately, we choose to show the result for the lowest speed value considered, as in this case the demands placed on the SAYDs to ensure vehicle stability are less severe, so there is room for the MPPT2 strategy to implement a reduction of the damping force through the opening of the commanded proportional valve. This behaviour is actually observed in the time history of the valve current: we consider first the case when the valve command starts at 0% (fully closed valve, blue line). The command rapidly increases to approximately 25% in the first 5 seconds of the simulation, then increases further to 35% approximately, showing that the controller settles to a condition of partial opening of the valves in the SAYDs. In case the command starts at 100% (fully open valve, red line) the command is rapidly decreased so that in the first 5 seconds of the simulation gets to 25-30% approximately, then follows the same trend of the case with initial 0% opening. The damper force is shown in Figure 14 and, consistently to the scope of the MPPT2 control strategy, is slightly reduced compared to the case of the MPPT1 strategy (see Figure 12), especially in terms of its high-frequency components which are relevant to noise transmission to the car body.

In conclusion, it can be stated that both the MPPT1 and MPPT2 strategies are fully effective with improving vehicle stability so that the vehicle's critical speed is raised above 400 km/h whilst for the vehicle with passive yaw dampers a critical speed of approximately 330 km/h is obtained. The MPPT2 strategy is also capable of accounting for reduced demand placed on the SAYDs at lower vehicle speed, whilst the MPPT1 strategy only aims at improving vehicle stability and hence tends to work always close to the maximum damping configuration of the SAYDs.

5.2.3 EMU vehicle with SAYD controlled by on-off skyhook strategy

The skyhook version of the control strategy aims at emulating the effect of a viscous damper connecting the bogie frame to a fixed point and the SAYD is switched between two opposite configurations, corresponding to the minimum and maximum opening of the valve.

Figure 15 shows the trend with speed of the dominant frequency and filtered RMS of the track shift forces and lateral bogie frame acceleration. The results show that also for this control strategy the vehicle is stable up to 400 km/h and above with very low RMS values both in terms of the track shift forces and bogie accelerations control strategy.

Figure 16 shows the time history of the valve current for the simulation performed at 400 km/h. Repeated switching between the fully closed and fully open position is observed, which is consistent with the control strategy implemented. It is important to highlight that for a practical implementation of this control strategy a fast valve response is needed because the controller is requiring to the valve to move from almost opposite positions in a very short time (less than 0.1 s). It is also observed that the peak force generated by the damper is higher in this case compared to the MPPT control strategy and this is due to high-frequency components in the signal which might be responsible of increased vibration of the car body.
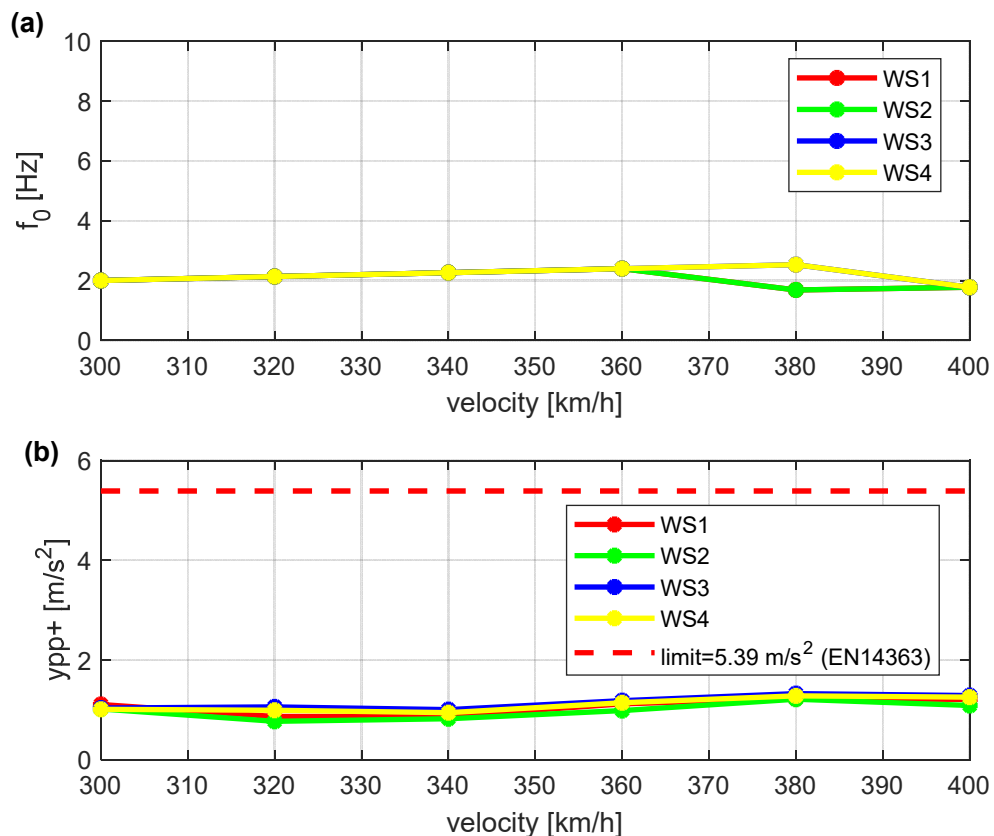

Figure 15 Dominant frequency (a), RMS of the acceleration of bogie frame (b) as function of vehicle velocity with on-off skyhook control
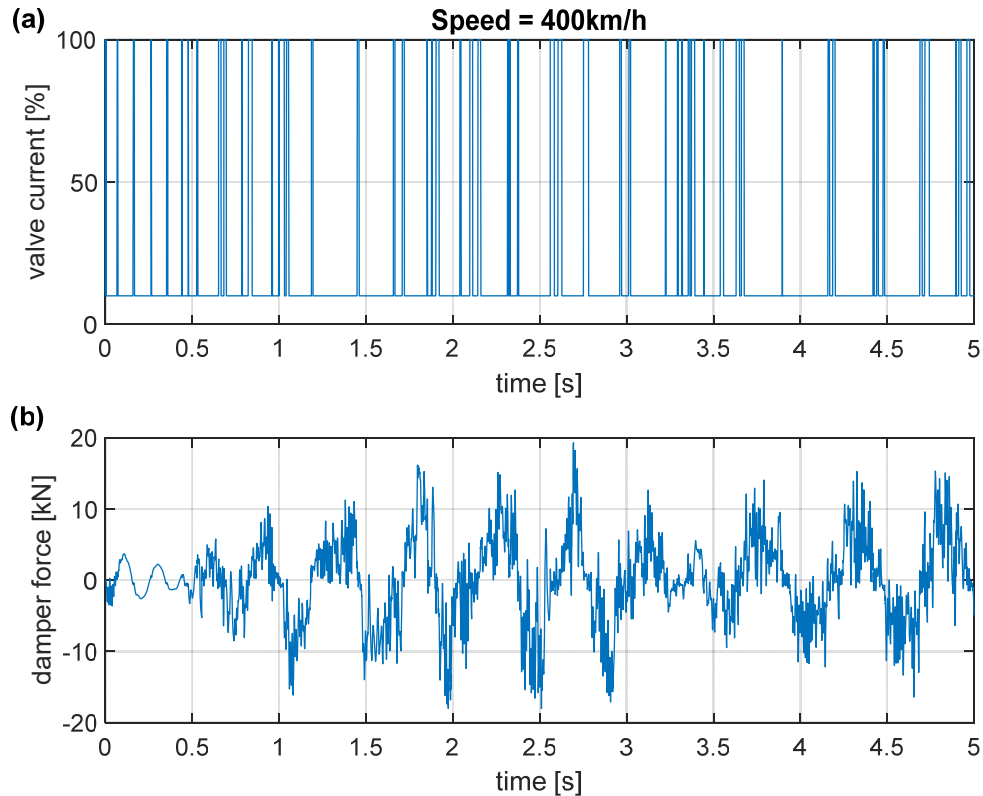
Figure 16 Time history of the valve current (a) and the force of SAYD (b) at speed 400km/h with on-off skyhook control.

5.2.4 EMU vehicle with SAYD controlled by continuous skyhook strategy

Finally, the last controller which was analysed is a different version of the skyhook control strategy, in which the partialisation of the SAYD valve is operated in continuous mode rather than in on-off mode.

Figure 17 show the trend with speed of the dominant frequency and filtered RMS of the track shift forces and lateral bogie frame acceleration. The results show once more that also using this control strategy the stability of the vehicle can be fully ensured in the entire range of speeds considered, although the RMS values are slightly higher than for the skyhook on-off strategy.

Figure 18 shows the time history of the valve current for the simulation performed at 400 km/h. Although the valve is in this case operated continuously, frequent switching between the slightly open position (10%) and fully open position is observed also in this case and thus again requiring fast variations of the controlled valve opening. The time history of the damper force is similar to the one obtained for the on-off skyhook strategy but shows even larger high-frequency contents which are undesired in view of the negative effect on car body vibration and interior noise.
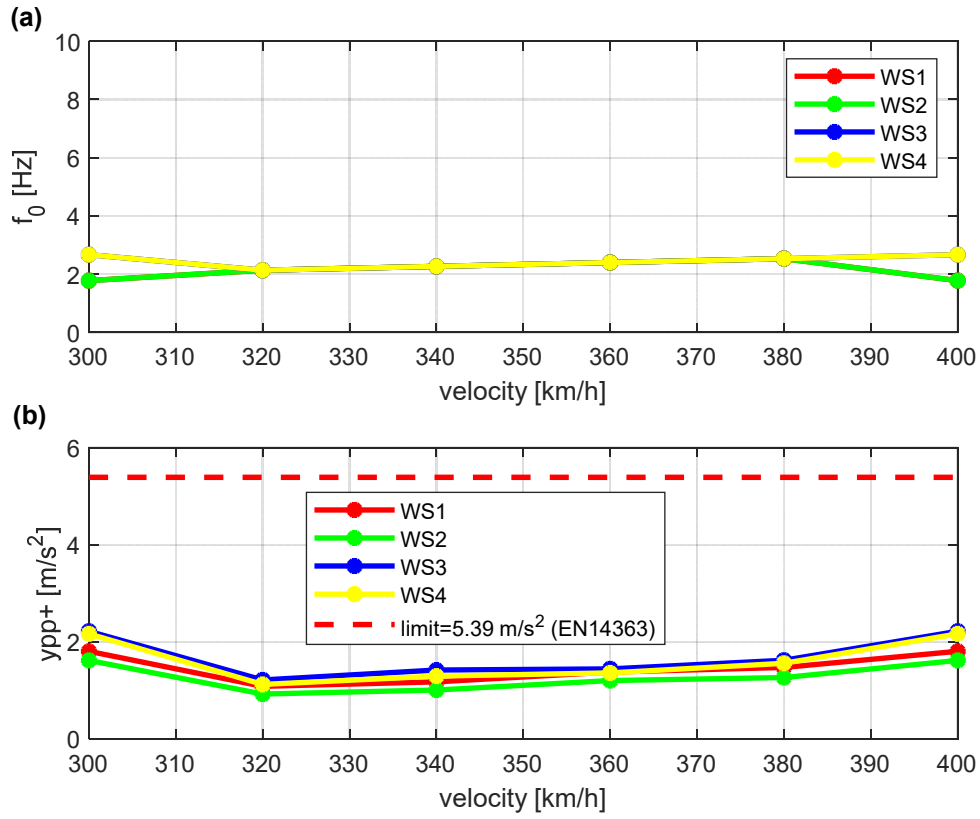
Figure 17 Dominant frequency (a), RMS of the acceleration of bogie frame (b) as function of vehicle velocity for EMU with SAYD controlled by continuous skyhook strategy
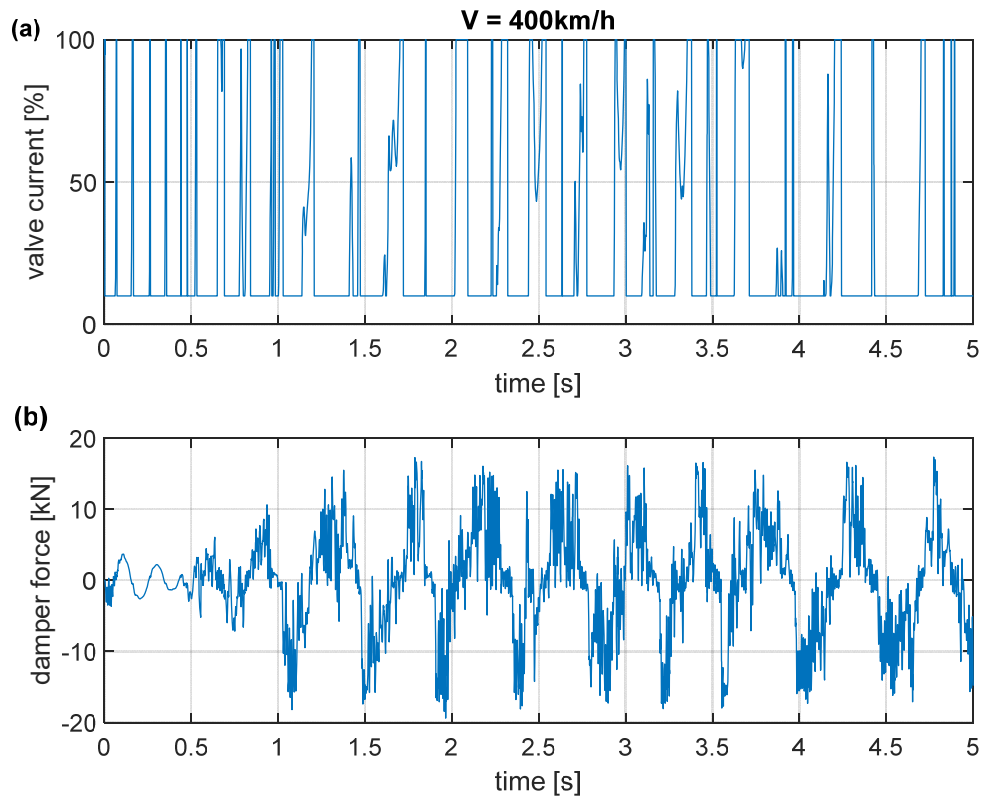
Figure 18 Time history of the valve current (a) and the force of SAYD (b) at speed 400km/h with continuous skyhook control

6   Conclusions

In this paper a concept for a hydraulic semi-active yaw damper (SAYD) is presented. This concept represents a further elaboration of Secondary Yaw Control for active stabilization of the bogie [2, 3] but envisages the use of semi-active hydraulic dampers instead of full-active electromechanical dampers, simplifying the design of the system and facilitating the design of a safe and fault tolerant device.

A co-simulation model was defined for a high speed vehicle equipped with the proposed SAYDs and numerical simulations were sed to assess the effect of the proposed SAYD concept in terms of improving vehicle stability and adapting damper behaviour to different running conditions of the vehicle. The co-simulation model consists of a non-linear multibody model of the vehicle coupled to a multi-physics model of the semi-active damper presented in Section 3.

Two main control strategies are considered for the SAYD: the MPPT strategy performs an empirical search for the best working condition of the semi-active damper, considering the damper's performance in terms of lowering the lateral vibration of the bogie frame and, at the same time, reduce the demand of damping force in the damper. The other control strategy considered is the classical skyhook damping for a semi-active damper, considering an on-off and a proportional formulation. Two variants of the MPPT control strategy are presented: the first one (MPPT1) aims at maximizing the damper's performance whilst the second one (MPPT2) aims at a balance of damper's performance and reduction of damping force.

The results of simulations performed using the co-simulation model show that the use of the SAYDs in combination with any of the control strategies considered allows to improve substantially the stability of the vehicle, so that the non-linear critical speed is raised in all cases beyond 400 km/h which is the maximum vehicle speed considered in this work. The MPPT1 strategy is unable to release performance demands placed on the SAYDs, as its goal is just concerned with maximizing the stability of the vehicle. On the other hand, the MPPT2 strategy provides comparable results in terms of increased vehicle stability but is also capable of adapting to running conditions in which a lower damping effect is required from the SAYDs by opening the controlled valve thereby limiting the damping force in running conditions where the maximum damping effect is not required.

As far as the on-off and continuous skyhook control strategies are concerned, again a very good improvement of vehicle stability is observed from numerical simulations, but the need of very fast variation of valve opening needs to be carefully considered in view of increased performance requirements placed on the commanded valve which would inevitably reflect in a higher cost for the hardware, and also in view of the durability of the SAYD hardware.

7 References

[1]   Wickens A. Fundamentals of Rail Vehicle Dynamics. Fundam. Rail Veh. Dyn. 2003.

[2]   Braghin F, Bruni S, Resta F. Active yaw damper for the improvement of railway vehicle stability and curving performances: Simulations and experimental results. Veh. Syst. Dyn. 2006;

[3]   Diana G, Bruni S, Cheli F, et al. Active Control of the Running Behaviour of a Railway Vehicle: Stability and Curving Performances. Veh. Syst. Dyn. 2002;

[4]   Matsumoto A, Sato Y, Ohno H, et al. Curving performance evaluation for active-bogie-steering bogie with multibody dynamics simulation and experiment on test stand. Veh. Syst. Dyn. 2008.

[5]   Mazzola L, Alfi S, Bruni S. A Method to Optimize Stability and Wheel Wear in Railway Bogies. Int. J. Railw. 2010;3:95–105.

[6]   Mousavi Bideleh SM, Berbyuk V, Persson R. Wear/comfort Pareto optimisation of bogie suspension. Veh. Syst. Dyn. 2016;

[7]   Goodall RM, Ward CP, Prandi D, et al. Railway bogie stability control from secondary yaw actuators. Dyn. Veh. Roads Tracks - Proc. 24th Symp. Int. Assoc. Veh. Syst. Dyn. IAVSD 2015. 2016.

[8]   Michálek T, Zelenka J. Reduction of lateral forces between the railway vehicle and the track in small-radius curves by means of active elements. Appl. Comput. Mech. 2011;

[9]   Stribersky A, Kienberger A, Wagner G, et al. Design and evaluation of a semi-active damping system for rail vehicles. Veh. Syst. Dyn. 1998;

[10]   O'Neill HR, Wale GD. Semí-actíve suspension improves rail vehicle ride. Comput.

Control Eng. J. 1994;

[11]   Lau YK, Liao WH. Design and analysis of magnetorheological dampers for train suspension. Proc. Inst. Mech. Eng. Part F J. Rail Rapid Transit. 2005;219:261–276.

[12]   Wang DH, Liao WH. Semi-active suspension systems for railway vehicles using magnetorheological dampers. Part I: System integration and modelling. Veh. Syst. Dyn. 2009;

[13]   Di Gialleonardo E, Braghin F, Bruni S. The influence of track modelling options on the simulation of rail vehicle dynamics. J. Sound Vib. [Internet]. 2012;331:4246–4258. Available   from: http://www.scopus.com/inward/record.url?eid=2-s2.0-84893845223&partnerID=MN8TOARS.

[14]   Alonso A, Giménez JG, Gomez E. Yaw damper modelling and its influence on railway dynamic stability. Veh. Syst. Dyn. 2011;

[15]   EN 14363. Railway applications — Testing and Simulation for the acceptance of running characteristics of railway vehicles — Running Behaviour and stationary tests. Communities. 2016.

[16]   Bruni S, Goodall R, Mei TX, et al. Control and monitoring for railway vehicle dynamics. Veh. Syst. Dyn. [Internet]. 2007 [cited 2018 Feb 20];45:743–779. Available from: http://www.tandfonline.com/doi/abs/10.1080/00423110701426690.

[17]   Savaresi S, Poussot-Vassal C, Spelta C, et al. Semi-Active Suspension Control Design for Vehicles. Semi-Active Suspens. Control Des. Veh. 2010.

[18]   Faranda R, Leva S. Energy comparison of MPPT techniques for PV Systems. WSEAS Trans. power Syst. 2008;

[19]   Karnopp D, Crosby MJ, Harwood RA. Vibration control using semi-active force generators. J. Manuf. Sci. Eng. Trans. ASME. 1974;

[20]   Esram T, Chapman PL. Comparison of photovoltaic array maximum power point tracking techniques. IEEE Trans. Energy Convers. 2007;

[21]   Reza Reisi A, Hassan Moradi M, Jamasb S. Classification and comparison of maximum power point tracking techniques for photovoltaic system: A review. Renew. Sustain. Energy Rev. 2013.

[22]   Margolis DL, Tylee JL, Horvat D. Heave mode dynamics of a tracked air cushion vehicle with semiactive airbag secondary suspension. J. Dyn. Syst. Meas. Control. Trans. ASME. 1975;97:399–407.

[23]   Sohn HC, Hong KS, Hedrick JK. Semi-active control of the Macpherson suspension system: hardware-in-the-loop simulations. IEEE Conf. Control Appl. - Proc. 2000.

[24]   Sammier D, Sename O, Dugard L. Skyhook and H∞ control of semi-active suspensions: Some practical aspects. Veh. Syst. Dyn. 2003;

[25]   Polach O. On non-linear methods of bogie stability assessment using computer simulations. Proc. Inst. Mech. Eng. Part F J. Rail Rapid Transit. 2006;

[26]   Alfi, S., Mazzola, L. and Bruni, S., Effect of motor connection on the critical speed of high-speed railway vehicles, Vehicle System Dynamics, 46:1, 201 — 214, 2008.